

Sequence Generation via Subsequence Similarity: Theory and Application to UAV Identification

Amir Kazemi

*National Center for Supercomputing Applications
University of Illinois at Urbana-Champaign
Urbana, IL, USA
kazemi2@illinois.edu*

Salar Basiri

*Department of Mechanical Engineering
University of Illinois at Urbana-Champaign
Urbana, IL, USA
sbasiri2@illinois.edu*

Volodymyr Kindratenko

*National Center for Supercomputing Applications
University of Illinois at Urbana-Champaign
Urbana, IL, USA
kindrtnk@illinois.edu*

Srinivasa Salapaka

*Department of Mechanical Engineering
University of Illinois at Urbana-Champaign
Urbana, IL, USA
salapaka@illinois.edu*

Abstract—The ability to generate synthetic sequences is crucial for a wide range of applications, and recent advances in deep learning architectures and generative frameworks have greatly facilitated this process. Particularly, unconditional one-shot generative models constitute an attractive line of research that focuses on capturing the internal information of a single image or video to generate samples with similar contents. Since many of those one-shot models are shifting toward efficient non-deep and non-adversarial approaches, we examine the versatility of a one-shot generative model for augmenting whole datasets. In this work, we focus on how similarity at the subsequence level affects similarity at the sequence level, and derive bounds on the optimal transport of real and generated sequences based on that of corresponding subsequences. We use a one-shot generative model to sample from the vicinity of individual sequences and generate subsequence-similar ones and demonstrate the improvement of this approach by applying it to the problem of Unmanned Aerial Vehicle (UAV) identification using limited radio-frequency (RF) signals. In the context of UAV identification, RF fingerprinting is an effective method for distinguishing legitimate devices from malicious ones, but heterogeneous environments and channel impairments can impose data scarcity and affect the performance of classification models. By using subsequence similarity to augment sequences of RF data with a low ratio (5%-20%) of training dataset, we achieve significant improvements in performance metrics such as accuracy, precision, recall, and F1 score.

Index Terms—Data augmentation, Synthetic Data, Generative Models, One-shot Learning, Drone, RF Signal.

I. INTRODUCTION

Synthetic data generation is a crucial field of study in machine learning and data science, with potential applications spanning a diverse array of disciplines. In many cases, obtaining large amounts of high-quality, labeled data is a significant challenge, and this scarcity can lead to biased or skewed results when training models [2]. Data generation methods can help create edge cases, rare events, and other scenarios that

are difficult to collect in real-world circumstances, allowing for more robust model training [3]. Additionally, to address privacy concerns, synthetic data mimics the characteristics of real data without revealing any sensitive information [4].

Sequences describe myriad of real-world data including image, video, audio, text, spatial and/or temporal physical state. For the technical and practical reasons just mentioned, generating synthetic sequences has gained unprecedented attention in the past decade. This is largely due to the recent advances in convolutional and recurrent neural networks (CNN and RNN) [5]–[8] as well as deep generative frameworks such as generative adversarial networks (GAN) [9] and variational autoencoder (VAE) [10]. The unconditional generation of sequences has been facilitated through the extension of such implicit models (i.e. GAN or VAE) to CNN, RNN, or a hybrid of both depending on the type of sequence (e.g. image or text) and the task [11]–[14].

The mentioned architectures and frameworks share deep neural networks (DNN) at their core. Training generalizable DNNs by Empirical Risk Minimization (ERM) [15], however, may breach the purpose if we resort to *data-intensive* deep generative models to address *data scarcity* (rather to preserve data privacy). On one hand, a variant of ERM, namely Vicinal Risk Minimization (VRM), allows for data augmentation where synthetic samples may be drawn from the vicinity of existing ones to expand the support of training data [16]. On the other hand, recent one-shot generative models [17]–[20], which can be non-deep [21]–[23], generate patch-similar images and videos from a single target. Considering the patch-similarity as a vicinity measure, one may therefore explore the ability of one-shot generative models for augmenting a whole dataset inspired by the VRM principle.

The motivation just described urges us to study how the similarity at the subsequence level affects the similarity at the sequence level. Particularly, we derive bounds on the distance of distributions for real and generated sequences based on that

This work utilizes resources supported by the National Science Foundation’s (NSF) Major Research Instrumentation Program, grant No. 1725729, as well as the University of Illinois at Urbana-Champaign [1].

of corresponding subsequences. To this end, we use a one-shot generative model to sample from the vicinity of individual sequences and generate subsequence-similar ones; see Fig. 1. Generated sequences can readily be fed into downstream tasks like classification to improve accuracy and other metrics, especially for low-data regime circumstances.

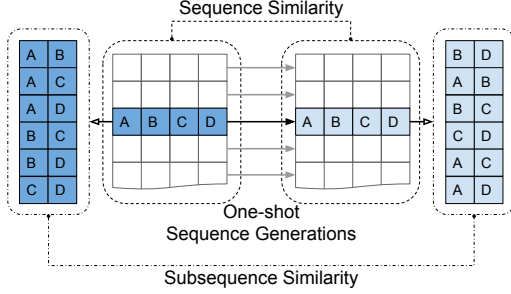


Fig. 1. A one-shot generative model is fed by real sequences (on left) to generate synthetic sequences (on right). Generating vicinal sequences is based on the similarity of subsequences. The metric for similarity is the optimal transport (Wasserstein distance between the distributions in this work).

Based on the provided theoretical support, we exploit subsequence-similarity for augmenting sequences and improving a classification task using synthetic data. To demonstrate the improvement, we apply the approach to the problem of Unmanned Aerial Vehicle (UAV) identification by limited radio-frequency (RF) signals. Similar to most cyber-physical systems, UAVs are prone to cyber-attacks, and RF fingerprinting helps distinguish legitimate devices from malicious ones in a reliable and effective manner. Therefore, RF-based UAV detection and identification have frequently been studied in recent years [24]–[27]. However, heterogeneous environment and channel impairment impose data scarcity on the classification model and affects its performance against adversarial examples [28]. In this work, we employ subsequence-similarity to augment sequences of transformed RF signals using a low ratio (5%-20%) of training data. The results demonstrate a significant improvement in performance metrics (accuracy, precision, recall, and F1 score) for the UAV identification.

The work is therefore structured as follows: First, we rigorously investigate the ability of one-shot generative models for augmenting a dataset of sequences. Particularly, we provide the mathematical definition of sequence, subsequence, one-shot generative models, and distance metrics. Then we derive the Wasserstein distance between the real and generated sequences based on that of subsequences. We also validate our general guarantee by intuitive special cases of sequences and subsequences. Second, we go through the UAV identification experiment and elaborate on the dataset, the selected one-shot generative model, the classification model, and the evaluation method. Finally, we discuss the results which include the accuracy, precision, recall, and F1-score of the classification task for all designed cases.

II. SEQUENCE AND SUBSEQUENCE SIMILARITY

As mentioned above, recent one-shot generative models for images and videos have become efficient thanks to avoiding deep neural networks and adversarial training. According to Fig 1, those models are indeed capable of data augmentation; however, such potential requires a guarantee as follows.

One-shot generative models optimize the similarity of patches between the target and the generated image, video, and other types of sequences. We may treat such data as sequences and their patches as substrings, or generally subsequences. Therefore, we define sequences, and projections in the first place; see Fig. 2. Let $\mathbf{V} \in \mathbb{R}^d$ represent a sequence, then $\mathbf{LV} \in \mathbb{R}^{d'}$ is a subsequence of length $d' \leq d$ with corresponding projection as $\mathbf{L}^T \mathbf{LV} \in \mathbb{R}^d$, where the linear transformation \mathbf{L} is a $d' \times d$ binary matrix defined as follows:

Definition 1. Let \mathbf{L} be a logical matrix in the probability space $(\Omega_L, \mathcal{F}_L, P_L)$ where the sample space Ω_L is

$$\Omega_L = \{\mathbf{L} | \mathbf{L} \in \{0, 1\}^{d' \times d}, \forall i, j \leq d : (\mathbf{L}^T \mathbf{L})_{ij} \leq (\mathbf{I})_{ij}\}, \quad (1)$$

\mathbf{I} is the identity matrix, and the event space \mathcal{F}_L is the set of all subsets of Ω_L , i.e. $\mathcal{F}_L = 2^{\Omega_L}$. The probability measure P_L is defined as follows:

$$P_L(\mathbf{L}) = \frac{\mathbf{1}_{f_L}(\mathbf{L})}{|f_L|} \quad (2)$$

where $\mathbf{1}_{f_L}(\mathbf{L}) = [\mathbf{L} \in f_L]$ is the indicator function, $f_L \subseteq \mathcal{F}_L$ and f_L^* is the set of all subsequences of length d' . Also, for every $\mathbf{V} \in \mathbb{R}^d$, f_L must satisfy:

$$\mathbf{V} = \sum_{\mathbf{L} \in f_L} \mathbf{L}^T \mathbf{LV} \oslash \mathbf{\Lambda}(f_L), \quad (3)$$

where \oslash denotes Hadamard division and

$$\mathbf{\Lambda}(f_L) = \sum_{\mathbf{L} \in f_L} \mathbf{L}^T \mathbf{1}_{d' \times 1}. \quad (4)$$

The definition states that we may use a subset (f_L) of all subsequences (f_L^*) to recover the sequence \mathbf{V} from projections using Eq. 3, but every element of the sequence \mathbf{V} must exist in at least one subsequence (or projection). This implies that $\mathbf{\Lambda}(f_L) \in \mathbb{N}^d$, as $\mathbf{\Lambda}(f_L)$ is simply the number of repetitions of elements of \mathbf{V} in subsequences; see Fig. 2. Based on this definition, we may now define the behavior of a one-shot generative model which generates subsequence-similar sequences for every target sequence in the dataset.

Definition 2 (One-shot Generative Model). Let \mathbf{X} be a d -dimensional sequence on $(\Omega_x \subset \mathbb{R}^d, \mathcal{B}(\Omega_x), P_X)$, \mathbf{Z} be a noise on $(\Omega_z \subset \mathbb{R}^d, \mathcal{B}(\Omega_z), P_Z)$, $G(\mathbf{X}, \mathbf{Z})$ be a generated sequence with $G : \mathbb{R}^d \times \mathbb{R}^d \rightarrow \mathbb{R}^d$ as the generative function, and \mathcal{B} be the Borel σ -algebra. Also, let σ, σ' be permutation functions belonging to the group of all permutations of the set f_L , i.e. $\sigma, \sigma' \in S_{|f_L|}$. Then, we assume that $\forall \mathbf{X} \in \Omega_x$, $\sigma, \sigma' \in S_{|f_L|}$, $\delta > 0$, there exists $\mathbf{Z} \in \Omega_z$ such that $G(\mathbf{X}, \mathbf{Z})$ admits the following property:

$$\inf_{\gamma \in \Gamma_0} \mathbf{E}_X \mathbf{E}_{(\sigma, \sigma') \sim \gamma} \|\sigma(\mathbf{L})\mathbf{X} - \sigma'(\mathbf{L})G(\mathbf{X}, \mathbf{Z})\| \leq \delta \quad (5)$$

where, by Def. 1, we have $\mathbf{E}_L[A(\mathbf{L})] = |f_L|^{-1} \sum_{\mathbf{L} \in f_L} A(\mathbf{L})$ for any mapping A , and Γ_0 is the set of joint distributions whose marginal probabilities are P_σ and $P_{\sigma'}$.

The recent definition simply states that for every target sequence \mathbf{X} in the dataset, the generative model finds another sequence $G(\mathbf{X}, \mathbf{Z})$ whose subsequences $\sigma'(\mathbf{L})G(\mathbf{X}, \mathbf{Z})$ are similar to that of the target one $\sigma(\mathbf{L})\mathbf{X}$ in the distributional sense. Note that $\sigma(\mathbf{L})$ and $\sigma'(\mathbf{L})$ are logical matrices, similar to \mathbf{L} . We use this definition to derive sequence similarity of the target and generated dataset, but prior to that, the metric for distributional distance is defined as follows:

Definition 3 (Distance Metric for Distributions). *The Wasserstein distance between sequences is defined as:*

$$W(\mathbf{X}, \mathbf{X}') = \inf_{\gamma \in \Gamma_1} \mathbf{E}_{(X, X') \sim \gamma} \|\mathbf{X} - \mathbf{X}'\| \quad (6)$$

where $\|\cdot\|$ denotes the L1 norm throughout this work, and Γ_1 is the set of joint distributions whose marginal probabilities are P_X and $P_{X'}$. For notational brevity, $W(A, B)$ is being used instead of $W(P_A, P_B)$.

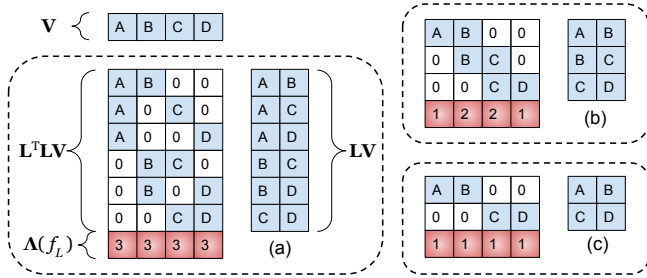


Fig. 2. Sequence \mathbf{V} , subsequence \mathbf{LV} , and projection $\mathbf{L}^T \mathbf{LV}$ for $d = 4$, $d' = 2$: (a) $f_L = f_L^*$ is the set of all subsequences of length $d' = 2$ which includes six subsequences, (b) and (c) $f_L \subset f_L^*$ is the set of substrings of length $d' = 2$.

The next two lemmas and theorem show that the optimal transport of target and synthetic sequences, using one-shot generative models, is bounded by the optimal transport of target and generated subsequences.

Lemma 1. $\forall \mathbf{X}, \mathbf{X}' \in \Omega_X, \mathbf{Z} \in \Omega_Z, \sigma, \sigma' \in S_{|f_L|}$ we have:

$$\begin{aligned} & \mathbf{E}_L \|\mathbf{L}^T \mathbf{LX}' - \mathbf{L}^T \mathbf{LG}(\mathbf{X}, \mathbf{Z})\| \\ & \leq \mathbf{E}_L \|\sigma(\mathbf{L})\mathbf{X} - \sigma'(\mathbf{L})\mathbf{X}'\| \\ & \quad + \mathbf{E}_L \|\sigma(\mathbf{L})\mathbf{X} - \sigma'(\mathbf{L})G(\mathbf{X}, \mathbf{Z})\| \end{aligned} \quad (7)$$

Proof. The triangle inequality gives:

$$\begin{aligned} & \mathbf{E}_L \|\sigma'(\mathbf{L})\mathbf{X}' - \sigma'(\mathbf{L})G(\mathbf{X}, \mathbf{Z})\| \\ & \leq \mathbf{E}_L \|\sigma(\mathbf{L})\mathbf{X} - \sigma'(\mathbf{L})\mathbf{X}'\| \\ & \quad + \mathbf{E}_L \|\sigma(\mathbf{L})\mathbf{X} - \sigma'(\mathbf{L})G(\mathbf{X}, \mathbf{Z})\| \end{aligned} \quad (8)$$

As subsequences in $\mathbf{E}_L \|\sigma'(\mathbf{L})\mathbf{X}' - \sigma'(\mathbf{L})G(\mathbf{X}, \mathbf{Z})\|$ are induced by the same permutation (i.e. σ'), with the abuse of notation, any permutation (say \mathbf{L}) can be used instead of $\sigma'(\mathbf{L})$. Also, the distance between subsequences induced

by the same permutation equals to the distance between corresponding projections. Therefore, we have:

$$\begin{aligned} & \mathbf{E}_L \|\sigma'(\mathbf{L})\mathbf{X}' - \sigma'(\mathbf{L})G(\mathbf{X}, \mathbf{Z})\| \\ & = \mathbf{E}_L \|\mathbf{L}^T \mathbf{LX}' - \mathbf{L}^T \mathbf{LG}(\mathbf{X}, \mathbf{Z})\| \end{aligned} \quad (9)$$

which proves the lemma. \square

Lemma 2. $\forall \mathbf{X}, \mathbf{X}' \in \Omega_X, \sigma, \sigma' \in S_{|f_L|}$, we have:

$$\begin{aligned} & \inf_{\gamma_1 \in \Gamma_1, \gamma_0 \in \Gamma_0} \mathbf{E}_{(X, X') \sim \gamma_1} \mathbf{E}_{(\sigma, \sigma') \sim \gamma_0} \\ & \mathbf{E}_L \|\sigma(\mathbf{L})\mathbf{X} - \sigma'(\mathbf{L})\mathbf{X}'\| = 0. \end{aligned} \quad (10)$$

Proof. Assuming the same probability space for $(\mathbf{X}, \mathbf{X}')$, and for (σ, σ') , we have $P_{X'} = P_X$ and $P_{\sigma'} = P_\sigma$, which is sufficient to prove the lemma. \square

Theorem 1. Assume that $\forall \mathbf{X}, \mathbf{X}' \in \Omega_X, \sigma, \sigma' \in S_{|f_L|}, \delta > 0$, there exists $\mathbf{Z} \in \Omega_Z$ such that: $\inf_{\gamma \in \Gamma_0} \mathbf{E}_X \mathbf{E}_{(\sigma, \sigma') \sim \gamma} \mathbf{E}_L \|\sigma(\mathbf{L})\mathbf{X} - \sigma'(\mathbf{L})G(\mathbf{X}, \mathbf{Z})\| \leq \delta$. Then we have

$$W(\mathbf{X}', G(\mathbf{X}, \mathbf{Z})) \leq (|f_L| / \min_i \Lambda_i(f_L)) \delta. \quad (11)$$

Proof. By definition in Eq (3), we have

$$\begin{aligned} & \|\mathbf{X}' - G(\mathbf{X}, \mathbf{Z})\| \\ & = \left\| \sum_{\mathbf{L} \in f_L} (\mathbf{L}^T \mathbf{LX}' - \mathbf{L}^T \mathbf{LG}(\mathbf{X}, \mathbf{Z})) \odot \Lambda(f_L) \right\| \end{aligned} \quad (12)$$

which, considering the fact that $\Lambda(f_L) \in \mathbb{N}^d$, it yields

$$\begin{aligned} & \|\mathbf{X}' - G(\mathbf{X}, \mathbf{Z})\| \\ & \leq (1 / \min_i \Lambda_i(f_L)) \left\| \sum_{\mathbf{L} \in f_L} (\mathbf{L}^T \mathbf{LX}' - \mathbf{L}^T \mathbf{LG}(\mathbf{X}, \mathbf{Z})) \right\| \\ & \leq (1 / \min_i \Lambda_i(f_L)) \sum_{\mathbf{L} \in f_L} \|\mathbf{L}^T \mathbf{LX}' - \mathbf{L}^T \mathbf{LG}(\mathbf{X}, \mathbf{Z})\| \\ & = (|f_L| / \min_i \Lambda_i(f_L)) \mathbf{E}_L \|\mathbf{L}^T \mathbf{LX}' - \mathbf{L}^T \mathbf{LG}(\mathbf{X}, \mathbf{Z})\| \end{aligned} \quad (13)$$

Using Lemma 1, we get

$$\begin{aligned} & \|\mathbf{X}' - G(\mathbf{X}, \mathbf{Z})\| \\ & \leq \left(\frac{|f_L|}{\min_i \Lambda_i(f_L)} \right) (\mathbf{E}_L \|\sigma(\mathbf{L})\mathbf{X} - \sigma'(\mathbf{L})G(\mathbf{X}, \mathbf{Z})\| \\ & \quad + \mathbf{E}_L \|\sigma(\mathbf{L})\mathbf{X} - \sigma'(\mathbf{L})\mathbf{X}'\|) \end{aligned} \quad (14)$$

but Lemma 2 and the theorem's assumption give

$$\inf_{\gamma \in \Gamma_1} \mathbf{E}_{(X, X') \sim \gamma} \|\mathbf{X}' - G(\mathbf{X}, \mathbf{Z})\| \leq \left(\frac{|f_L|}{\min_i \Lambda_i(f_L)} \right) (\delta + 0) \quad (15)$$

and proves the theorem:

$$W(\mathbf{X}', G(\mathbf{X}, \mathbf{Z})) \leq \left(\frac{|f_L|}{\min_i \Lambda_i(f_L)} \right) \delta. \quad (16)$$

\square

We may gain more insight from the bound in Eq. (11) if we consider special cases of f_L . In the next corollary, we will see the behavior of the bound for $f_L = f_L^*$ and, in the following corollary, we consider the two-dimensional case of sequences. The latter is critical for using existing generative models, as

most of them are designed for two-dimensional arrays (such as images).

Corollary 1. Assume that $\forall \mathbf{X}, \mathbf{X}' \in \Omega_X$, $\sigma, \sigma' \in S_{|f_L|}, \delta > 0$, there exists $\mathbf{Z} \in \Omega_Z$ such that: $\inf_{\gamma \in \Gamma_0} \mathbf{E}_X \mathbf{E}_{(\sigma, \sigma') \sim \gamma} \mathbf{E}_L \|\sigma(\mathbf{L})\mathbf{X} - \sigma'(\mathbf{L})G(\mathbf{X}, \mathbf{Z})\| \leq \delta$. Then, if $f_L = f_L^*$ we have

$$W(\mathbf{X}', G(\mathbf{X}, \mathbf{Z})) \leq \left(\frac{d}{d'}\right) \delta. \quad (17)$$

Proof. If f_L equals the set of all subsequences of length d' , i.e. f_L^* , then we have

$$|f_L| = \binom{d}{d'}, \quad \Lambda(f_L) = \binom{d-1}{d'-1} \mathbf{1}^{d \times 1}. \quad (18)$$

Therefore, Theorem 1 gives

$$W(\mathbf{X}', G(\mathbf{X}, \mathbf{Z})) \leq \left(\frac{\binom{d}{d'}}{\binom{d-1}{d'-1}}\right) \delta = \left(\frac{d}{d'}\right) \delta \quad (19)$$

which proves the corollary. The result is intuitive, because as the length of subsequences d' tends to the length of the sequence d , the bound on the distributional distance of sequences and subsequences matches each other, i.e. δ . \square

Corollary 2. Assume that $\forall \mathbf{X}, \mathbf{X}' \in \Omega_X$, $\sigma, \sigma' \in S_{|f_L|}, \delta > 0$, there exists $\mathbf{Z} \in \Omega_Z$ such that: $\inf_{\gamma \in \Gamma_0} \mathbf{E}_X \mathbf{E}_{(\sigma, \sigma') \sim \gamma} \mathbf{E}_L \|\sigma(\mathbf{L})\mathbf{X} - \sigma'(\mathbf{L})G(\mathbf{X}, \mathbf{Z})\| \leq \delta$. Let $\mathbf{X} = \text{vec}(\mathbf{Y})$ where \mathbf{Y} belongs to $(\Omega_Y \subset \mathbb{R}^{n \times n}, \mathcal{B}(\Omega_Y), P_Y)$. Then, if f_L denotes the set of all $n' \times n'$ substrings where $n' \leq n$, we have following bounds:

$$W(\mathbf{X}', G(\mathbf{X}, \mathbf{Z})) \leq (n - n' + 1)^2 \delta, \quad (20)$$

and

$$W(\mathbf{X}', G(\mathbf{X}, \mathbf{Z})) \leq \left(1 + \frac{n-1}{n'}\right)^2 \delta. \quad (21)$$

Proof. If f_L equals the set of all $n' \times n'$ substrings, then we have

$$|f_L| = (n - n' + 1)^2, \quad \min_i \Lambda_i(f_L) = 1. \quad (22)$$

Therefore, Theorem 1 gives

$$W(\mathbf{X}', G(\mathbf{X}, \mathbf{Z})) \leq \left(\frac{(n - n' + 1)^2}{1}\right) \delta = (n - n' + 1)^2 \delta \quad (23)$$

which proves Eq. (20). The result is intuitive, because as the dimensions of substring $(n' \times n')$ tend to that of the sequence $(n \times n)$, the bound on the distributional distance of sequences and substrings matches each other, i.e. δ . See Fig. 3.

Although the bound in Eq. (20) is asymptotically intuitive (i.e. when $n' \rightarrow n$), we may obtain a tighter bound as follows. It is evident that the previous bound suffers from $\min_i \Lambda_i(f_L) = 1$. Alternatively, we may perform optimal transport on zero-padded data pairs, as zero elements do not contribute to the cost of transport between the distributions (Fig. 4). On one hand, zero-padding a length of $n' - 1$ per each side of \mathbf{Y} , gives $\min_i \Lambda_i(f_L) = n'^2$ for the set of non-padded elements. On the other hand, $\Lambda_i(f_L)$ can be assumed to have

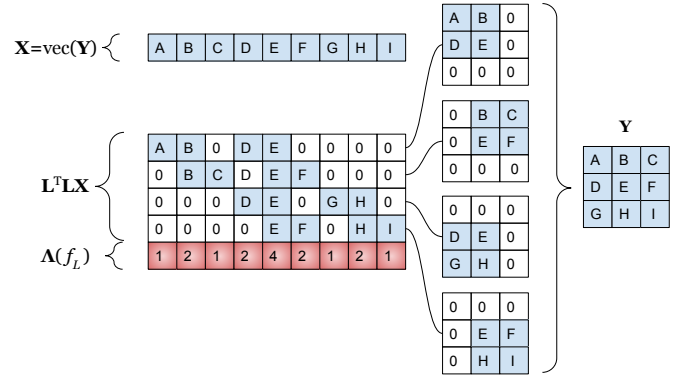


Fig. 3. An $n \times n$ matrix \mathbf{Y} with $n' \times n'$ substrings, vectorized as sequence \mathbf{X} with projections as $\mathbf{L}^T \mathbf{L} \mathbf{X}$, where $n = 3$ and $n' = 2$.

any (non-zero) value for the set of zero-padded elements as they do not contribute to the optimal transport. Therefore, for the padded \mathbf{Y} we have:

$$|f_L| = (n + n' - 1)^2, \quad \min_i \Lambda_i(f_L) = n'^2; \quad (24)$$

which, using Theorem (1), gives:

$$W(\mathbf{X}', G(\mathbf{X}, \mathbf{Z})) \leq \left(\frac{(n + n' - 1)^2}{n'^2}\right) \delta = \left(1 + \frac{n-1}{n'}\right)^2 \delta. \quad (25)$$

For $1 < n' < n - 1$, Eq. (21) gives a tighter bound compared with Eq. (20). While for $n' = 1$ and $n' = n - 1$ both give $n^2 \delta$ and 4δ as the upper bounds, respectively, Eq. (20) is tighter only for the asymptotic case of $n' = n$.

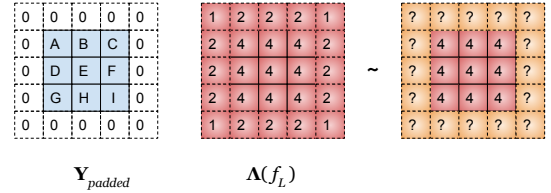


Fig. 4. Zero-padded \mathbf{Y} is $(n + 2n' - 2) \times (n + 2n' - 2)$, where $n = 3$ and $n' = 2$. The central $n \times n$ elements are repeated n' times each. The repetition of other elements can be substituted arbitrarily (marked by ?), as corresponding elements in \mathbf{Y}_{padded} are zero in both real and generated data and do not contribute to optimal transport.

\square

III. EXPERIMENT

Based on the guarantees derived in the previous section, we examine the ability of a one-shot generative model for generating synthetic datasets. Particularly, we evaluate the performance improvement of a classification task using synthetic data. To this aim, we randomly sample the original training data to reduce the sample size, then apply a one-shot generative model to the individual samples of reduced datasets to generate a synthetic dataset of the original size. Finally, we train a DNN on the original, reduced, and synthetic datasets,

evaluate the network on the test dataset (which is unseen for all the cases), and compare the performance metrics.

A. Dataset

In this paper, we use the drone Radio Frequency (RF) dataset developed in [24] where the authors have collected and processed RF signals of three different types of drones under various flight statuses¹. They have processed RF signals using Fourier transform to obtain frequency content for detection and identification purposes: detect the presence of a drone (two classes), detect the presence of a drone and identify its type (four classes), and detect the presence of a drone and identify its type as well as its flight mode (10 classes). In this work, we focus on the two latter cases. We use the preprocessed content of RF signals featured by 2025 points, which are reshaped as 45×45 matrices for the one-shot generation purpose based on the guarantee in Corollary 2. As we are concerned with low-regime data circumstances in this work, we have randomly down-sampled this dataset from 22700 to 1135 according to the proportion of each label. We call this $1135 \times 45 \times 45$ dataset the original one throughout this work. Also, each sample is associated with a label which is a one-hot encoded vector of size 4 or 10, depending on the desired classification task. The first class in each task is the background noise for no-UAV scenario.

Table I summarizes the specifications of the datasets used in this work for the 4-classes and 10-classes tasks. We first randomly sample 20% of the original dataset for testing (verification) purposes, none of which is used in any training, hence can be used to assess different scores of the trained model against adversarial samples. The remaining data are used for training, which consist of 908 samples in total. Then, the size of each randomly sampled (reduced) dataset is reported, for four cases of 5, 10, 15, and 20% of the original data. The label breakdown of each dataset is also shown in the multi-column below each dataset in each row; for instance, in the 4-classes task (C4), the first class in the original data has 164 samples, the second class has 336 samples, the third has 324 and the fourth class has 84 samples, where all added together compose the entire 908 samples. The same convention is applied to the 10-classes task (C10), where the label breakdown is presented for the 10-classes (in three rows, where the no-UAV class corresponds to the top left cell). Using the reduced datasets, we generate synthetic ones as many as the size of the original one (i.e. 908), as this helps to have a fair comparison of the performance between the models trained by synthetic and original data.

B. One-shot Generative Model

The approach in Fig. 1 is based on one-shot generative models. Corollary 2 guarantees that one-shot generation of sequences (as reshaped two-dimensional arrays or images) augments the whole dataset. Therefore, we may exploit existing single image generation architectures for this purpose,

by using the reshaped samples as 45×45 images, rather than sequences of length 2025. Such a reshaping is for the generative model and is reserved in the next step for the classification task.

In this work, we use the algorithm in [22], namely Generating by Patch Distribution Matching (GPDM), which is based on minimizing the Wasserstein distance between the patches of real and generated images. The algorithm also utilizes a multi-scale hierarchical strategy to learn the global structure of the image in the early stages of training. The hyper-parameters for GPDM in this work are as follows: *finest scale* = 45×45 , *coarsest scale* = 21×21 , *patch size* = 11×11 , *decrease rate of scales* = 0.95, *number of projections for sliced Wasserstein distance* = 128, *learning rate* = 0.02, and finally *iteration steps* = 300.

C. Classification Models

In this paper, we use a Deep Neural Network (DNN) structure to classify the input data. The network has three inner layers, each having 128 neurons excluding bias, and their activation function is Rectified Linear Unit (ReLU). The input layer of the network has the same size as the input data, as shown in Table I. The outer layer has a dimension of 4 or 10 (depending on the task) and a sigmoid activation function. An ADAM optimizer with a learning rate of 0.0001 is used to optimize the parameters of the network. To avoid overfitting, we use an Early Stopping mechanism to keep track of the training loss, and terminate the training process if no improvement is observed in the training loss for n consecutive samples, where n is chosen to be 2% of the training size. Lastly, the batch size of training is five.

D. Evaluation method

The evaluation is conducted on eight tasks: 4-classes and 10-classes UAV (and flight mode) identification, each having four cases of generation on 5, 10, 15, and 20% of the original data. For each case, we use a randomly sampled 5-fold cross-validation [29] setting and report the average scores over all of the folds.

Four metrics are used to evaluate classification using the eight cases of generated data. As we are dealing with a multi-label classification problem, the following scores are calculated for each label, then are averaged by the weight of their support (the number of true instances for each label). Denote the number of true positive, true negative, false positive, and false negative data as TP , TN , FP , and FN , respectively. By definition, we have:

$$\begin{aligned} \text{Accuracy} &= (TP + TN) / (TP + TN + FP + FN) \\ \text{Precision} &= TP / (TP + FP) \\ \text{Recall} &= TP / (TP + FN) \\ F_1 &= 2 \times (\text{Precision} \times \text{Recall}) / (\text{Precision} + \text{Recall}) \end{aligned} \quad (26)$$

Fig. 5 shows an overview of the evaluation flow we used to assess the performance of our data generation module. The raw RF dataset is first down-sampled and pre-processed to generate the modified dataset. Then, a 5-fold cross-validation

¹<https://github.com/AI-Sad/DroneRF>

TABLE I
NUMBER OF DATA SAMPLES FOR EACH DATASET TYPE IN THE 4-CLASSES (C4) AND 10-CLASSES (C10) TASKS. RED. AND SYNTH. REPRESENT REDUCED AND SYNTHETIC DATASETS RESPECTIVELY.

Data/ Size	Original				Red. (5%)				Red. (10%)				Red. (15%)				Red. (20%)				Synth.
Train	908				46				91				152				182				908
C4	164	336	324	84	9	16	17	4	17	33	33	8	28	56	54	14	33	67	65	17	
C10	164	84	84	84	9	4	4	4	17	8	9	8	28	14	14	14	33	17	17	17	
	84	84	84	84	4	5	4	4	8	9	8	9	14	14	14	14	16	17	17	17	
	72	84	-		4	4	-		7	8	-		12	14	-		14	17	-		
Test	227																				

is applied to the modified dataset to randomly select data samples for the original train set and the test set. The first DNN is trained on the original train set. In the next step, the second DNN is trained on a reduced-size train set, which is generated by randomly sampling the original train set. This step is done for four cases of 5, 10, 15, and 20% sampling ratios. The reduced datasets are fed to the synthesizer module, and synthetic datasets are generated and provided to the third DNN for training. Finally, all of the DNNs are evaluated on the test set, and the whole process is repeated over all of the folds for both tasks of 4 and 10-classes. The results are the average values over all folds.

IV. RESULTS AND DISCUSSION

Generation of synthetic sequences based on subsequence similarity is guaranteed according to Section II. To demonstrate the bound in Eq. (21), we plot the ratio of $W(\mathbf{X}', G(\mathbf{X}, \mathbf{Z}))$ to δ against n'/n , in comparison with the bound $(1 + (n-1)/n')^2$; see Fig 6, where generation is based on the highest scale, i.e. $n = 45$, and patch or substring dimensions as follows $n' = \{5 : 5 : 40\}$. Note that δ is obtained using the equality case of Eq. (5). As expected, the ratio of $W(\mathbf{X}', G(\mathbf{X}, \mathbf{Z}))$ to δ tends to one by increasing the dimension of patches. This ratio is subject to approximations, because we estimate high-dimensional distributional distances (both W and δ) by the sliced Wasserstein distance whose accuracy is affected by the number of samples as well as by the number of patches within each sample.

For the multiscale generation setup, described in Section III.B, we can visualize the generated data (blue) versus the original one (red) by t-SNE for different patch dimensions; see Fig. 7. We only present patches with a dimension less than 21, as the lowest scale of generation is 21×21 according to the mentioned setup. As can be seen, increasing the patch dimension provides a higher fidelity for the generation as samples get closer to each other. However, for the sake of diversity, we choose 11×11 patches to provide the classifier with more adversarial samples.

The classification results are presented in Fig. 8 where we see the average and standard deviation for different scores, reported for all of the tasks and datasets. The labels on the x-axis represent the number of classes (following 'C') and the reduced size as the percentage of original data (following 'P'). For example, 'C10P05' denotes the 10-classes task while the size of reduced data is 5% of the original one. The y-axis denotes the score value. In the reduced datasets, especially for the 5% and 10% cases, the size of training data becomes significantly limited for each label (see Table I). Therefore, we would like to investigate the performance of DNN trained on a dataset that is synthesized from such a limited number of samples.

The accuracy plot suggests that relying on subsequence similarity for sequence generation provides adequate training data to train an accurate classifier. The accuracy gap between

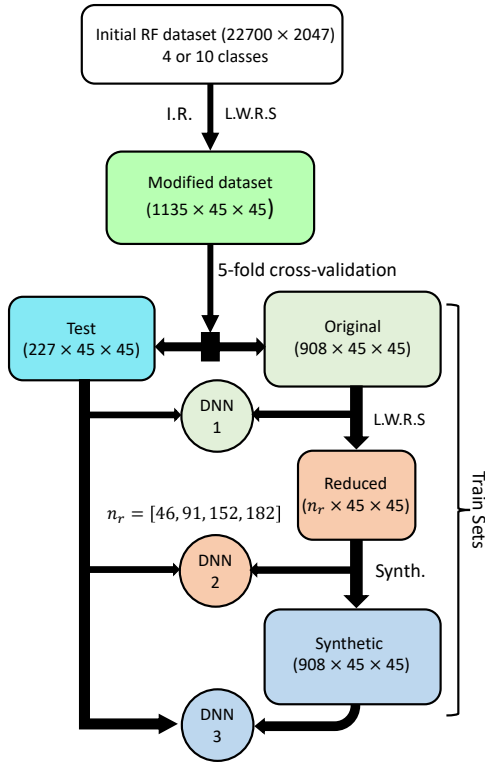


Fig. 5. A schematic of the evaluation mechanism of this paper. L.W.R.S, I.R., and Synth. stand for label-weighted random sampling, image representation, and synthesizer respectively. Here n_r is the sample size of the reduced dataset.

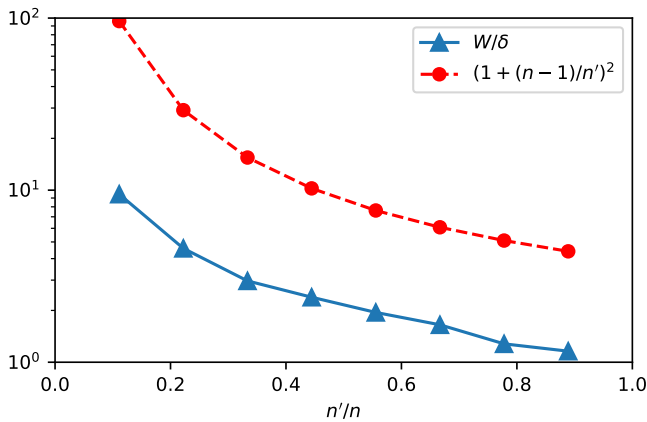


Fig. 6. Demonstration of Eq. (21) where generation is based on $n = 45$ and patch or substring dimensions are $n' = \{5 : 5 : 40\}$.

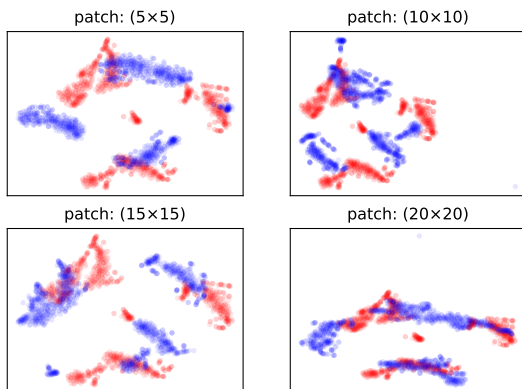


Fig. 7. Visualization of the generated data (blue) versus the original one (red) by t-SNE for different patch dimensions using GPDM with hyperparameters described in Section III.B.

the synthetic dataset and the reduced dataset is remarkably large for the 5% and 10% cases, implying that the approach can perform accurately for simulating features, or spectral behavior, in extremely low-data regime circumstances. The gap shrinks as we use more samples of the original data for generation; see C10P20 and C04P20 cases. As expected, the test accuracy of DNNs on synthetic data rarely exceeds that of the original data, at least when both datasets have the same size.

As Fig. 8 shows, models trained on reduced datasets lose their precision significantly, especially in the case of 5% and 10% where the loss of precision is in orders of magnitude. Synthetic training datasets, on the contrary, have significantly higher precision which is attributed to the usage of a one-shot generative model. As mentioned before, inspired by the VRM principle, we search the vicinity of existing samples to generate new ones which tend to be a precise sampling.

The recall plot also demonstrates an improvement for all

cases using synthetic training datasets. One may sacrifice fidelity (precision) for diversity (recall) by tuning hyperparameters of the one-shot generative model (GPDM) differently (see section III-B). We, however, prefer to improve precision more than recall for classification purposes, as too diverse synthetic data may mislead the classifiers.

Finally, the F1 plot shows similar results to previous metrics, as the F1-score of the classification using reduced datasets is significantly less than that of the original and synthetic ones, especially in the 5% and 10% cases. The difference between the accuracy and F1-score is mainly because the latter does not involve TN.

V. CONCLUSION

In conclusion, the ability to generate synthetic sequences has gained significant attention in the past decade due to advances in CNNs and RNNs, as well as deep generative frameworks such as GANs and VAEs. These architectures and frameworks share DNN at their core, so the data-intensive deep generative models fail to address extreme data scarcity issues. Inspired by the VRM principle, one-shot generative models offer a potential solution to the problem by allowing for data augmentation. In this work, we studied the effect of similarity at the subsequence level on the similarity at the sequence level, deriving bounds on the optimal transport of real and generated sequences. We then applied this approach to the problem of UAV identification by extremely limited RF signals and demonstrated a significant improvement in performance metrics when using synthetic data. Overall, this research highlights the potential of using subsequence-similarity to augment sequences and improve the performance of classification tasks in low-data regime circumstances.

ACKNOWLEDGMENT

Amir Kazemi appreciates discussions with Hadi Meidani, as well as NSF's NCSA Internship Program for Cyberinfrastructure Professionals, grant No. 1730519 [30].

REFERENCES

- [1] V. Kindratenko, D. Mu, Y. Zhan, J. Maloney, S. H. Hashemi, B. Rabe, K. Xu, R. Campbell, J. Peng, and W. Gropp, "Hal: Computer system for scalable deep learning," in *Practice and Experience in Advanced Research Computing*, 2020, pp. 41–48.
- [2] S. I. Nikolenko, *Synthetic data for deep learning*. Springer, 2021, vol. 174.
- [3] D. Libes, D. Lechevalier, and S. Jain, "Issues in synthetic data generation for advanced manufacturing," in *2017 IEEE International Conference on Big Data (Big Data)*. IEEE, 2017, pp. 1746–1754.
- [4] H. B. McMahan, D. Ramage, K. Talwar, and L. Zhang, "Learning differentially private recurrent language models," *arXiv preprint arXiv:1710.06963*, 2017.
- [5] W. Rawat and Z. Wang, "Deep convolutional neural networks for image classification: A comprehensive review," *Neural computation*, vol. 29, no. 9, pp. 2352–2449, 2017.
- [6] J. Gu, Z. Wang, J. Kuen, L. Ma, A. Shahroudy, B. Shuai, T. Liu, X. Wang, G. Wang, J. Cai *et al.*, "Recent advances in convolutional neural networks," *Pattern recognition*, vol. 77, pp. 354–377, 2018.
- [7] Y. Yu, X. Si, C. Hu, and J. Zhang, "A review of recurrent neural networks: Lstm cells and network architectures," *Neural computation*, vol. 31, no. 7, pp. 1235–1270, 2019.
- [8] A. Graves, "Generating sequences with recurrent neural networks," *arXiv preprint arXiv:1308.0850*, 2013.

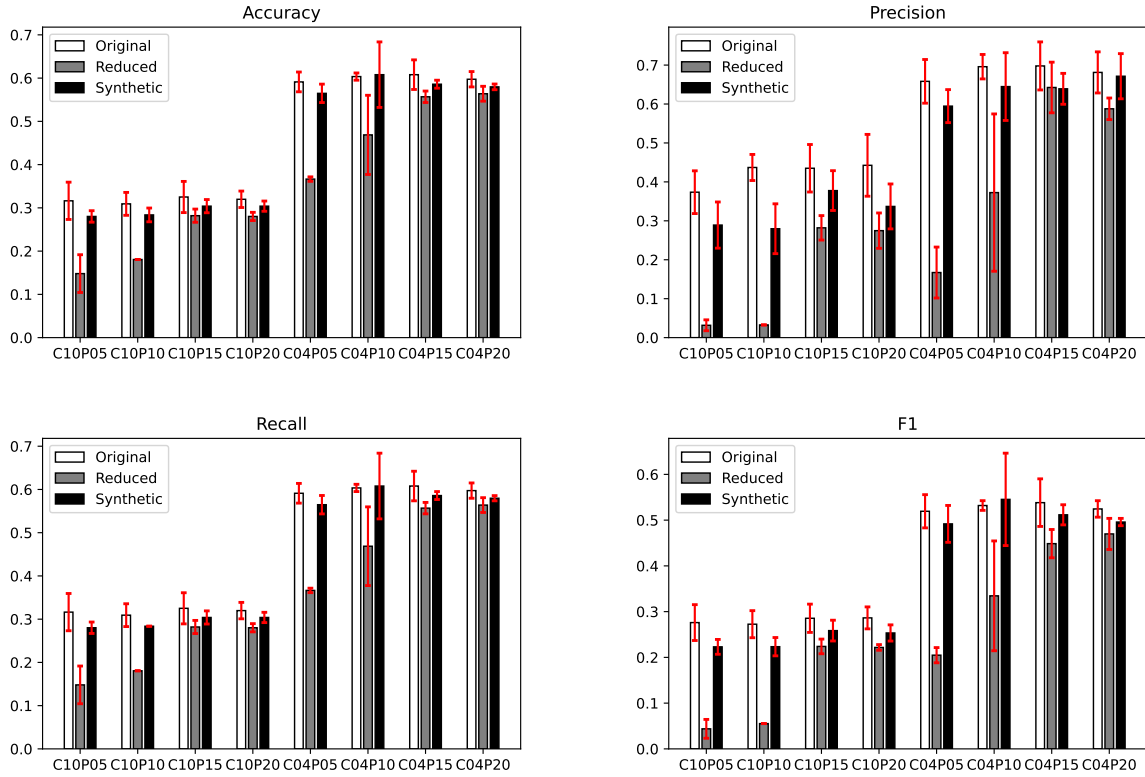


Fig. 8. Average and standard deviation of different metrics shown for all of the datasets and tasks.

- [9] I. Goodfellow, J. Pouget-Abadie, M. Mirza, B. Xu, D. Warde-Farley, S. Ozair, A. Courville, and Y. Bengio, "Generative adversarial networks," *Communications of the ACM*, vol. 63, no. 11, pp. 139–144, 2020.
- [10] D. P. Kingma and M. Welling, "Auto-encoding variational bayes," *arXiv preprint arXiv:1312.6114*, 2013.
- [11] J. Chung, K. Kastner, L. Dinh, K. Goel, A. C. Courville, and Y. Bengio, "A recurrent latent variable model for sequential data," *Advances in neural information processing systems*, vol. 28, 2015.
- [12] L. Yingzhen and S. Mandt, "Disentangled sequential autoencoder," in *International Conference on Machine Learning*. PMLR, 2018, pp. 5670–5679.
- [13] J. Han, M. R. Min, L. Han, L. E. Li, and X. Zhang, "Disentangled recurrent wasserstein autoencoder," *arXiv preprint arXiv:2101.07496*, 2021.
- [14] O. Mogren, "C-rnn-gan: Continuous recurrent neural networks with adversarial training," *arXiv preprint arXiv:1611.09904*, 2016.
- [15] H. Zhang, M. Cisse, Y. N. Dauphin, and D. Lopez-Paz, "mixup: Beyond empirical risk minimization," *arXiv preprint arXiv:1710.09412*, 2017.
- [16] O. Chapelle, J. Weston, L. Bottou, and V. Vapnik, "Vicinal risk minimization," *Advances in neural information processing systems*, vol. 13, 2000.
- [17] T. R. Shaham, T. Dekel, and T. Michaeli, "Singan: Learning a generative model from a single natural image," in *Proceedings of the IEEE/CVF International Conference on Computer Vision*, 2019, pp. 4570–4580.
- [18] A. Shocher, S. Bagon, P. Isola, and M. Irani, "Ingan: Capturing and re-targeting the "dna" of a natural image," in *Proceedings of the IEEE/CVF International Conference on Computer Vision*, 2019, pp. 4492–4501.
- [19] T. Hinz, M. Fisher, O. Wang, and S. Wermter, "Improved techniques for training single-image gans," in *Proceedings of the IEEE/CVF Winter Conference on Applications of Computer Vision*, 2021, pp. 1300–1309.
- [20] Y. M. Asano, C. Rupprecht, and A. Vedaldi, "A critical analysis of self-supervision, or what we can learn from a single image," *arXiv preprint arXiv:1904.13132*, 2019.
- [21] N. Granot, B. Feinstein, A. Shocher, S. Bagon, and M. Irani, "Drop the gan: In defense of patches nearest neighbors as single image generative models," in *Proceedings of the IEEE/CVF Conference on Computer Vision and Pattern Recognition*, 2022, pp. 13 460–13 469.
- [22] A. Elnekave and Y. Weiss, "Generating natural images with direct patch distributions matching," *arXiv preprint arXiv:2203.11862*, 2022.
- [23] N. Haim, B. Feinstein, N. Granot, A. Shocher, S. Bagon, T. Dekel, and M. Irani, "Diverse generation from a single video made possible," in *European Conference on Computer Vision*. Springer, 2022, pp. 491–509.
- [24] M. F. Al-Sa'd, A. Al-Ali, A. Mohamed, T. Khattab, and A. Erbad, "Rf-based drone detection and identification using deep learning approaches: An initiative towards a large open source drone database," *Future Generation Computer Systems*, vol. 100, pp. 86–97, 2019.
- [25] W. Nie, Z.-C. Han, M. Zhou, L.-B. Xie, and Q. Jiang, "Uav detection and identification based on wifi signal and rf fingerprint," *IEEE Sensors Journal*, vol. 21, no. 12, pp. 13 540–13 550, 2021.
- [26] I. Nemer, T. Sheltami, I. Ahmad, A. U.-H. Yasar, and M. A. Abdeen, "Rf-based uav detection and identification using hierarchical learning approach," *Sensors*, vol. 21, no. 6, p. 1947, 2021.
- [27] R. Wang, Z. Li, J. Tang, and H. Wen, "Rf fingerprint identification of commercial uav in outdoor environment," in *2022 International Conference on Computing, Communication, Perception and Quantum Technology (CCPQT)*. IEEE, 2022, pp. 367–371.
- [28] O. M. Gul, M. Kulhandjian, B. Kantarci, A. Touazi, C. Ellement, and C. D'Amours, "Fine-grained augmentation for rf fingerprinting under impaired channels," in *2022 IEEE 27th International Workshop on Computer Aided Modeling and Design of Communication Links and Networks (CAMAD)*. IEEE, 2022, pp. 115–120.
- [29] X. Zeng and T. R. Martinez, "Distribution-balanced stratified cross-validation for accuracy estimation," *Journal of Experimental & Theoretical Artificial Intelligence*, vol. 12, no. 1, pp. 1–12, 2000.
- [30] D. Lapine, V. Kindratenko, and L.-M. Rosu, "Ncsa internship program for cyberinfrastructure professionals," in *Practice and Experience in Advanced Research Computing*, 2020, pp. 414–420.

APPENDIX

To analyze the performance of classification tasks, we have presented the confusion matrices as well. Table II shows confusion matrices for the 4- and 10-classes tasks trained on the original, reduced (5%), and synthetic datasets. The first column and row in each confusion matrix corresponds to the label number, and each row represents the predicted label, while each column represents the ground truth label. Therefore, the diagonal values represent the accuracy of the model for each label, and the average of all of the diagonal values is equal to the total accuracy of the model reported in Fig. 8. These confusion matrices help us to identify which labels are most confused with other labels on the test dataset. This table suggests that the DNN models trained on the synthetic data have a quite similar classification behavior to the models trained on the original datasets, while the classification performance of the models trained on reduced datasets radically deteriorates. Using synthetic datasets, however, the classification accuracy is recovered over most of the labels, leading to an overall accuracy close to the original model.

TABLE II
CONFUSION MATRICES FOR THE CLASSIFICATION OF THE ORIGINAL, REDUCED, AND SYNTHETIC DATASETS SHOWING THE AVERAGE ACCURACY VALUES ON DIFFERENT LABELS (TOP AND BOTTOM MATRICES CORRESPOND TO THE 4-CLASSES AND 10-CLASSES SCENARIO, RESPECTIVELY. EACH COLUMN REPRESENTS THE GROUND TRUTH LABEL AND EACH ROW REPRESENTS THE PREDICTED LABEL.

	0	1	2	3
0	0.99	0.00	0.00	0.01
1	0.00	0.76	0.24	0.00
2	0.00	0.71	0.29	0.00
3	0.03	0.52	0.12	0.32

	0	1	2	3	4	5	6	7	8	9
0	0.99	0.00	0.00	0.00	0.00	0.00	0.00	0.00	0.00	0.00
1	0.01	0.01	0.05	0.20	0.36	0.00	0.19	0.17	0.00	0.01
2	0.00	0.01	0.02	0.17	0.40	0.00	0.21	0.17	0.02	0.00
3	0.00	0.01	0.00	0.20	0.42	0.00	0.19	0.16	0.02	0.00
4	0.00	0.01	0.01	0.21	0.36	0.01	0.18	0.20	0.02	0.00
5	0.00	0.01	0.00	0.17	0.36	0.08	0.17	0.17	0.04	0.00
6	0.00	0.01	0.00	0.06	0.35	0.00	0.33	0.16	0.04	0.05
7	0.00	0.00	0.01	0.09	0.38	0.00	0.31	0.11	0.03	0.07
8	0.00	0.00	0.00	0.14	0.32	0.03	0.21	0.18	0.11	0.00
9	0.03	0.00	0.00	0.12	0.26	0.00	0.13	0.18	0.00	0.28

a) Original

	0	1	2	3
0	0.00	0.80	0.20	0.00
1	0.00	0.78	0.22	0.00
2	0.00	0.79	0.21	0.00
3	0.00	0.80	0.20	0.00

	0	1	2	3	4	5	6	7	8	9
0	0.60	0.00	0.00	0.00	0.20	0.00	0.00	0.00	0.00	0.20
1	0.59	0.00	0.00	0.00	0.21	0.02	0.00	0.00	0.00	0.18
2	0.57	0.00	0.00	0.00	0.23	0.00	0.00	0.00	0.00	0.20
3	0.59	0.00	0.00	0.00	0.21	0.00	0.00	0.00	0.00	0.20
4	0.58	0.00	0.00	0.00	0.22	0.01	0.00	0.00	0.00	0.19
5	0.60	0.00	0.00	0.00	0.20	0.01	0.00	0.00	0.00	0.19
6	0.58	0.01	0.00	0.00	0.21	0.00	0.00	0.00	0.00	0.20
7	0.60	0.00	0.00	0.00	0.20	0.00	0.00	0.00	0.00	0.20
8	0.59	0.00	0.00	0.00	0.21	0.00	0.00	0.00	0.00	0.20
9	0.59	0.00	0.00	0.00	0.21	0.00	0.00	0.00	0.00	0.20

b) Reduced

	0	1	2	3
0	0.97	0.01	0.00	0.01
1	0.00	0.56	0.44	0.00
2	0.00	0.54	0.45	0.00
3	0.11	0.41	0.26	0.22

	0	1	2	3	4	5	6	7	8	9
0	0.97	0.00	0.00	0.00	0.00	0.00	0.01	0.00	0.01	0.00
1	0.00	0.00	0.00	0.00	0.00	0.73	0.04	0.00	0.06	0.17
2	0.00	0.02	0.02	0.00	0.00	0.70	0.02	0.00	0.04	0.20
3	0.00	0.01	0.01	0.00	0.00	0.70	0.02	0.00	0.06	0.20
4	0.00	0.01	0.01	0.00	0.02	0.73	0.03	0.00	0.04	0.16
5	0.01	0.00	0.00	0.00	0.01	0.73	0.04	0.00	0.03	0.18
6	0.01	0.02	0.00	0.00	0.00	0.70	0.04	0.02	0.02	0.19
7	0.00	0.00	0.00	0.00	0.00	0.73	0.03	0.01	0.03	0.20
8	0.01	0.00	0.00	0.00	0.00	0.61	0.10	0.00	0.11	0.17
9	0.12	0.00	0.00	0.00	0.00	0.61	0.02	0.02	0.00	0.23

c) Synthetic